

# Dense Indoor mmWave Wearable Networks: Managing Interference and Scalable MAC

Yicong Wang and Gustavo de Veciana

Department of Electrical and Computer Engineering, The University of Texas at Austin

Email: yicong.wang@utexas.edu, gustavo@ece.utexas.edu

**Abstract**—MmWave based wearable networks will need to function in various environments including possibly high density settings, e.g., train cars. At such densities one might expect challenges in interference management and/or excessive overheads tracking and jointly scheduling interferers. In this paper we use simple stochastic geometric models to examine the characteristics (number and sensitivity to motion) of “strong interferers” and show that due to blocking they are not monotonic in user density. Indeed, perhaps surprisingly, the most challenging setting appears to arise at “intermediate” user densities. We then propose a simple model to evaluate the performance of current MAC designs based on clustering and hierarchical scheduling. The results exhibit a performance trade-off leading to an optimal cluster size which depends on the directionality of transmissions. More importantly, we show that at high densities the per user throughput is roughly constant, suggesting wearable networks will scale well in dense scenarios.

## I. INTRODUCTION

The market for wearable devices is growing quickly and research on possible types of wearable networks is actively being pursued [1]. In the future, users may be equipped with multiple on body interconnected devices, some of which may require high bandwidth, e.g., devices supporting high quality audio/video and delivering augmented reality experiences. To support such high data rates and operate at possibly high user densities, millimeter wave (mm-wave) communication in the 60GHz band has been proposed and standards developed for short-range wireless personal area networks (WPAN), e.g., 802.11ad [2], 802.15.3c [3] and ECMA387 [4].

Signal propagation in the mm-wave band is different from bands traditionally used for mobile wireless devices. The free space path loss in the mm-wave band is higher, thus the transmission range is short, and mm-wave transmissions experience higher loss due to blockage. This makes the transmissions depend mostly on the availability of a line-of-sight (LOS) channel or strong reflected non-line-of-sight (NLOS) channel. Further, the human body introduces a path loss of over 20dB [5] thus movements of a user and its neighbors may greatly change the channels. Devices operating in the mm-wave band usually use directional transmissions and reception, thus the antenna gain is non-uniform. As a result, the channels in the mm-wave band are very sensitive to the environment and user motions. These characteristics are not necessarily shortcomings, e.g., short range, directionality and blockage can reduce the interference seen at receivers, naturally simplifying interference management. In this paper we focus on dense indoor environments with possibly very high user densities and

dynamics, e.g., a crowded train car. Such a setting corresponds to one of the extreme environments where the technology should operate seamlessly. It is an open question if and how the MAC protocols should adapt to work in such environments.

Another key characteristic of mm-wave wearable networks is the possible heterogeneity of devices. Wearable devices may have different transmission capabilities in terms of beam-forming/directionality, computation capacity, transmit power and energy, etc. Moreover, the traffic patterns of users/devices may be different, some may leverage highly directional links between smart phones and augmented reality devices while other users may have multiple low-end devices with relatively poor directionality. Such heterogeneity makes it challenging to optimize MAC protocols to guarantee Quality-of-Service (QoS) requirements for high-end applications.

The above characteristics affect MAC design in different ways. The nature of mm-wave propagation makes it possible to achieve higher spatial reuse, but scheduling users is challenging as the signaling can be unreliable and the interference characteristics may change frequently. The high density of users and user dynamics in indoor environments suggest that the MAC protocols should coordinate among users using limited signaling to reduce overheads. Heterogeneity of devices may require transmissions be treated differently and the MAC should adapt to different devices and QoS requirements.

*Contributions.* In this paper, we explore the nature of mm-wave propagation for dense wearable networks to better understand the role of interference and the need for coordination and MAC scheduling in such environments.

We first study the characteristics, i.e., number, location and sensitivity to motion, of “strong interferers” as seen by a typical receiver in a dense wearable environment. The strong interferers are those that in principle a MAC protocol would aim to address through scheduling. We note that some work has been done on analyzing the signal-to-interference-ratio (SINR) distribution in dense wearable networks but the studies mostly assume there is no scheduling or consider simple protocols like Aloha [6][7]. Our main findings regarding the interference environment include:

- The average number of strong interferers seen by a typical receiver does not keep increasing with user density. In fact it reaches a peak then starts decreasing as a result of human body blockage.

- In highly dense environments, most strong interferers are actually nearby since the close neighbors essentially form a “ring” round the user blocking more distant interferers.
- Strong interferers are most sensitive to users’ local motions at intermediate user densities.

We then revisit current approaches to MAC design for wearable networks which leverage clustering and hierarchical scheduling and study their performance in high density scenarios given the particular characteristics of mm-wave propagation discussed above. Our main contributions and findings regarding MAC and scheduling with clustering include:

- We propose a simple model to analyze the performance of clustering and scheduling for dense wearable networks and validate it through simulation.
- We explore the trade-offs associated with cluster size: large clusters reduce inter-cluster interference but require more coordination overheads and result in reduced reuse versus small clusters.
- We study how the transmission capabilities of devices impact the best cluster size: highly directional transmissions prefer smaller cluster sizes while low directional transmissions prefer larger clusters to mitigate interference. MAC schedulers can and should be optimized depending on device transmission capabilities and QoS requirements.
- We show that the *per user throughput* first decreases with user density as expected, but then remains stable and even increases at high densities. The optimal cluster size also remains roughly constant in dense scenarios. Our results suggest that, perhaps surprisingly, the MAC of wearable networks is “scalable” to high user densities.

*Related work.* The channel and interference characteristics in the mm-wave band have been studied in [8] for urban cellular network and [6][7] for indoor wearable networks. In these works, the transmissions of users are not coordinated, or assume simple protocols like Aloha, and the interference from all users is summed up to analyze the SINR. In this paper, instead, we focus on characterizing the set of users the MAC needs to coordinate so as to identify the requirements on the MAC. [9][10][11] study the impact of human mobility on the channel between two fixed points through measurements and simulations, but do not study how the set of interferers is affected.

MAC protocols have been proposed to improve the spatial reuse for mm-wave networks [12][13][14], but the characteristics in dense wearable networks, i.e., the blockage of user body and large density of devices, are not considered. The authors of [15] propose a link scheduling protocol for mm-wave ad hoc networks with blockage. However, the blockage model does not consider the actual characteristics of dense wearable networks, i.e., the parameters of channels are set without considering the blockage model, user density and locations of users.

*Organization.* In the next section, we discuss the system model used in our paper. We then present an analysis of

the number of strong interferers and their sensitivity to local motions in Section III. In Section IV we study the performance of clustering in hierarchical wearable MAC protocols. We conclude the paper in Section V.

## II. SYSTEM MODEL

In this section we introduce the system model for dense wearable networks. The devices on each user form a Personal Basic Service Set (PBSS), coordinated by the PBSS Control Point (PCP), e.g., the user’s smart phone. Data transmissions only happen between the PCP and non-PCP devices of the same PBSS. There is no access point (AP) or central controller to coordinate or synchronize transmission across all users. We use the channel between two PCPs to approximate the channels between the devices in two PBSSs. PCPs are located in the front of user body at a fixed height  $h_{\text{device}}$ , see Fig. 1. We define an interferer as a *strong interferer* if the interference power,  $P_r$ , exceeds a threshold  $\gamma_{\text{SI}}$ , i.e.,  $P_r > \gamma_{\text{SI}}$ , where

$$P_r = P_t \cdot G_t \cdot G_r \cdot L,$$

$P_t$  is the transmit power,  $G_t$  and  $G_r$  are the transmit and receive antenna gains, and  $L$  is the path loss.

**User model.** Users are assumed to stand on a 2-D plane. Walls and obstructions other than human bodies are not considered, but we shall assume there is a ceiling at a height  $h_{\text{ceiling}}$ . For simplicity, users’ bodies are of the same dimension.

Consider the user located at the origin 0 with an orientation  $\Theta_0$ , which is uniformly distributed on  $[0, 2\pi]$ . The centers of other users,  $\Phi = \{X_i\}$ , follow a homogeneous Poisson Point Process (HPPP) with intensity  $\lambda$ , conditioning on that there is no point on  $b(0, r_{\text{min}})$ . Here  $b(0, r_{\text{min}})$  denotes a disc centered at 0 with radius  $r_{\text{min}}$ , and  $r_{\text{min}}$  is the minimum distance between users. Let  $\Theta_i$  denote the orientation of user  $i$ , which is assumed to be independent and identically distributed (i.i.d.) and uniformly distributed on  $[0, 2\pi]$ .  $\tilde{\Phi} = \{(X_i, \Theta_i)\}$  is an independently marked point process (i.m.p.p.) and the network is uniquely defined by  $\tilde{\Phi}$ . We let  $\phi = \{(x_i, \theta_i)\}$  denote a realization of  $\tilde{\Phi}$ . We will use the location of user to represent the user, e.g.,  $x_i$  for user  $i$ .

**Channel model.** We use the location of the center of a user to approximate the location of the user’s PCP. Only two types of channel are considered, the LOS channel and the reflected channel over the ceiling, which we refer to as the NLOS channel. The LOS channel follows the free space propagation model while the path loss of the reflected channel is determined by the free space path loss and a ceiling reflection coefficient,  $\Gamma$ , which depends on incident angle and reflection material [16].

**Blockage model.** We assume that the channel gain of an interference channel is 0 if the channel is blocked by users, including self blockage. For self blockage, we assume user’s body would block both the LOS and NLOS channels to/from devices behind the user as shown in Fig. 1. We say that two users are “facing” each other if they are in the non self-block regions of each other.

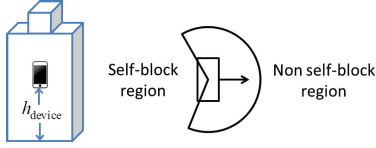


Fig. 1. Illustration of the location of PCP and self-blockage model. The PCP is located in front of user body at a height  $h_{\text{device}}$ . The arrow indicates the orientation of the user.

Blocking by other users can be different for LOS and NLOS channels. Consider the channel between the user at the origin and the user at location  $x$ , and a potential blocking user  $(x', \theta')$ , see Fig. 2(a). We assume user  $x'$  blocks the LOS channel if the following two conditions are met,

$$s_x(x') \in [0, |x|] \text{ and } 0 \in D_x(x, \theta'),$$

where  $s_x(x') \in \mathbb{R}$  is the projection of  $x'$  on the unit vector from 0 to  $x$ ,  $|x|$  is the distance between  $x$  and 0,  $D_x(x', \theta') \subset \mathbb{R}^2$  is the projection of user's cross section at height  $h_{\text{device}}$  on the vector  $n_x$ , which is the vector perpendicular to the vector from 0 to  $x$ . For blocking of the NLOS channel, we further assume that the cross section of the user body at height higher than the device,  $h \geq h_{\text{device}}$ , is contained in the cross section at height  $h_{\text{device}}$ . Thus  $x'$  blocks the NLOS channel if an additional third condition is satisfied:

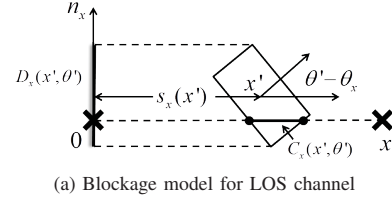
$$h_{\text{NLOS}}(x, s_x(x')) \leq h_{(x', \theta')}(y), \forall y \in C_x(x', \theta'),$$

where  $h_{\text{NLOS}}(x, s_x(x'))$  is the height of the NLOS channel at distance  $s_x(x')$  from 0 and  $h_{(x', \theta')}(y)$  is the height of user  $(x', \theta')$  at location  $y$ ,  $C_x(x', \theta') \subset \mathbb{R}^2$  is the intersection of the cross section of user  $(x', \theta')$  and the segment between 0 and  $x$ , see Fig. 2. This additional condition implies that if the LOS channel is not blocked, the NLOS channel is also not blocked.

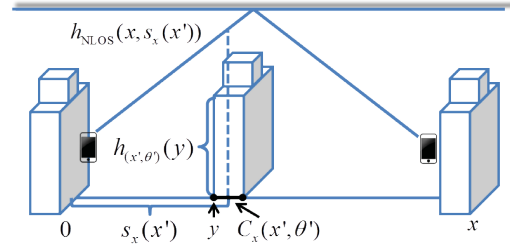
Given  $P_t$ ,  $G_t$  and  $G_r$ , let  $r_{\text{max}}$  be the maximum distance of a strong interferer when the LOS channel is available, and  $r_{\text{max}}^{\text{reflection}}$  that when the NLOS channel is not blocked but the LOS channel is blocked. Due to reflection loss and longer path,  $r_{\text{max}}^{\text{reflection}} < r_{\text{max}}$ . For  $|x| \in [r_{\text{min}}, r_{\text{max}}^{\text{reflection}}]$ , user  $x$  is a strong interferer if the NLOS channel is not blocked; for  $|x| \in (r_{\text{max}}^{\text{reflection}}, r_{\text{max}}]$ , user  $x$  is a strong interferer if the LOS channel is not blocked. Notice that the path loss of the NLOS channel may not be a monotonic increasing function of  $|x|$  due to the sensitivity of the reflection coefficient to incident angle, thus for  $|x| < r_{\text{max}}^{\text{reflection}}$ , having an unblocked NLOS channel is only a necessary condition for being a strong interferer in some scenarios. The model can be easily extended to account for these effects.

**Antenna model.** We assume that the antenna gain is invariant to the angle between antenna direction and the vertical axis, e.g., the same for the LOS and the NLOS channel between two devices. The antenna gain follows a sectorized antenna model, i.e.,

$$G = \begin{cases} g_{\text{main}}, & w.p. \beta/2\pi \\ g_{\text{side}}, & w.p. 1 - \beta/2\pi \end{cases},$$



(a) Blockage model for LOS channel



(b) Blockage model for NLOS channel

Fig. 2. (a) shows the conditions that user  $(x', \theta')$  blocks the LOS channel between 0 and  $x$ . (b) illustrate the additional condition required for NLOS channel.

where  $g_{\text{main}}$  is the antenna gain of main lobe,  $g_{\text{side}}$  is the antenna gain out of the main lobe,  $\beta$  is the beamwidth on the 2-D plane users are standing.

There are many complex factors involved in mm-wave propagation but the simple model captures the salient features for such systems.

### III. INTERFERENCE IN DENSE MM-WAVE WEARABLE NETWORKS

In this section we study the interference environment a user would experience in a dense mm-wave wearable network.

#### A. Number of Strong Interferers

We first analyze the number of strong interferers seen by the user at 0,  $(0, \theta_0)$ ,  $N_{\text{SI}}$ .  $N_{\text{SI}}$  can be written as follows,

$$N_{\text{SI}} = \sum_{(X, \Theta) \in \tilde{\Phi}} f(X, \Theta, \tilde{\Phi} \setminus \{(X, \Theta)\}, 0, \theta_0), \quad (1)$$

where  $f(X, \Theta, \tilde{\Phi} \setminus \{(X, \Theta)\}, X_0, \Theta_0)$  is the indicator function that user  $(X, \Theta)$  is a strong interferer of user  $(X_0, \Theta_0)$  given the other users,  $\tilde{\Phi} \setminus \{(X, \Theta)\}$ .

$N_{\text{SI}}$  is a function of  $\tilde{\Phi}$ , and this makes the distribution of  $N_{\text{SI}}$  hard to compute. Still the average number of strong interferers is a good metric to capture the MAC coordination requirements/overhead.

To compute  $E[N_{\text{SI}}]$  we first compute the probability that the channel between 0 and  $x$  is blocked. Denote by  $N_{\text{B}}^{\text{LOS}}(x)$  a random variable corresponding to the number of users blocking the LOS channel between 0 and  $x$ ,  $N_{\text{B}}^{\text{NLOS}}(x)$  a random variable corresponding to the number of users blocking the NLOS channel. Clearly  $N_{\text{B}}^{\text{NLOS}}(x) \leq N_{\text{B}}^{\text{LOS}}(x)$  almost surely according to our model. The distribution of  $N_{\text{B}}^{\text{LOS}}(x)$  is given in the following theorem.

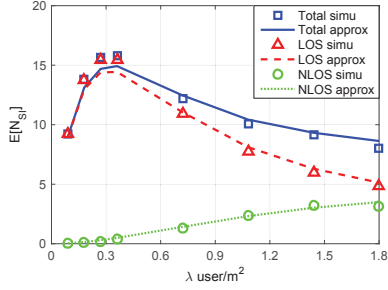


Fig. 3.  $E[N_{SI}]$  for different user densities.  $h_{\text{body}} = 1.754\text{m}$ ,  $h_{\text{device}} = 1\text{m}$ ,  $h_{\text{ceiling}} = 2.8\text{m}$ ,  $|\Gamma|^2 = 0.2166$ . PBSSs work on 60GHz band and the threshold of path loss for strong interferers is -88 dB,  $r_{\text{max}} = 10\text{m}$ , and  $r_{\text{max}}^{\text{reflection}} = 3.1\text{m}$ .

**Theorem 1.** *If user locations follow an HPPP with density  $\lambda$ ,  $N_B^{\text{LOS}}(x)$  follows a Poisson distribution with mean  $E[N_B^{\text{LOS}}(x)] \approx \lambda|x|E[D]$ , where  $E[D]$  is the expected width of a user's cross section at  $h_{\text{device}}$ . The probability that the LOS channel is not blocked is  $e^{-E[N_B^{\text{LOS}}(x)]}$ .*

The proof of Theorem 1 is based on showing that  $N_B^{\text{LOS}}(x)$  is obtained from a thinned Poisson process [17] and using Campbell's formula [18] to get its mean. For NLOS channels,  $N_B^{\text{NLOS}}(x)$  also follows Poisson distribution and its mean can be computed similarly.

Based on the above analysis and assumptions,  $E[N_{SI}]$  can be computed using the Reduced Campbell's formula for i.m.p.p. of Corollary 2.2 in [18] as follows,

$$E[N_{SI}] = P_{\text{facing}} \int_{R_0} [1(|x| \in [r_{\min}, r_{\max}^{\text{reflection}}]) \cdot e^{-E[N_B^{\text{NLOS}}(x)]} + 1(|x| \in (r_{\max}^{\text{reflection}}, r_{\max}) \cdot e^{-E[N_B^{\text{LOS}}(x)]}] \lambda(dx), \quad (2)$$

where  $P_{\text{facing}}$  is the probability that user  $x$  and user 0 faces each other,  $R_0 = \mathbb{R}^2 \setminus b(0, r_{\min})$ .

**Numerical results.** In a dense scenario, HPPP model for users locations may not be a good model as users can not overlap with each other and this may affect the accuracy of our model for  $E[N_{SI}]$ . In Fig. 3 we compare our analytical results with simulation accounting for user not overlapping. Users are modeled as cylinders with a diameter of 0.6m, and we use Matérn III process [19] to model user locations in a simulation with  $r_{\min} = 0.6\text{m}$ . Our analytical results are in line with the simulation, validating the accuracy of the approximation.  $E[N_{SI}]$  first grows with the user density, but as user density further increases, close neighbors block the interference from more distant users, thus  $E[N_{SI}]$  saturates and begins to decrease with density. Users see the largest number of strong interferers at moderately high user densities.

Fig. 4 illustrates the distribution for the distance of strong interferers for varying user densities. Fig. 5 shows the locations of strong interferers in one realization of the network. As user density increases, the strong interferers tend to concentrate close to the receiver. When user density is very high, the network reaches a ‘‘jamming regime’’, where strong interferers

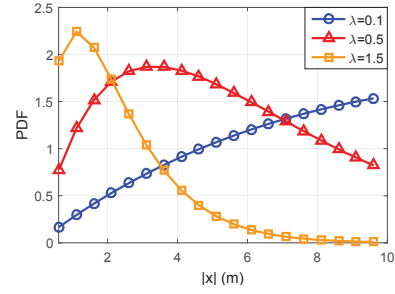


Fig. 4. Probability density function of LOS strong interferers as a function of the distance to the user at 0,  $|x|$ .

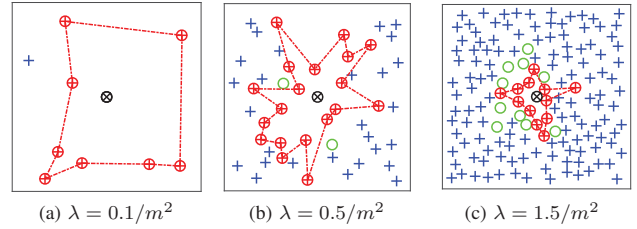


Fig. 5. The locations of strong interferers for different densities, ignoring self blockage. The joint red circles represent LOS interferers, green hollow circles are NLOS interferers and blue crosses are non strong interferers. The area shown above is  $10\text{m} \times 10\text{m}$ .

are mostly close by and block further away interferers as shown in Fig. 5(c).

### B. Sensitivity of Strong Interferers

In this section we study the sensitivity of strong interferers to users' small local movements. The sensitivity of strong interferers, i.e., how the set of strong interferers changes when users move, influences the cost and benefit of tracking and coordinating with such neighbors.

Suppose in a time interval  $[t, t + \Delta t]$ , users make independent small scale movements, i.e., translation  $\Delta X_i$  and rotation  $\Delta \Theta_i$ . Denote by  $\tilde{\Phi}^t$  the network at time  $t$ . Given  $\tilde{\Phi}^t = \tilde{\phi}^t$  and the user at 0 is  $(0, \theta_0)$  at  $t$ , the changes of the network are summarized as follows:

$$(0, \theta_0) \rightarrow (\Delta X_0, \theta_0 + \Delta \Theta_0),$$

$$\tilde{\phi}^t = \{(x_i, \theta_i)\} \rightarrow \tilde{\phi}^{t+\Delta t} = \{(x_i + \Delta X_i, \theta_i + \Delta \Theta_i)\}.$$

We assume both  $\Delta X_i$  and  $\Delta \Theta_i$  are i.i.d.,  $\Delta X_i$  is uniformly distributed in  $b(0, r_{\text{move}})$ ,  $r_{\text{move}}$  is the maximum range of movements,  $\Delta \Theta_i$  is uniformly distributed in  $[-\omega, \omega]$ .

Denote by  $Y_x^t = f(x, \Theta, \tilde{\Phi}^t \setminus (x, \Theta), 0, \Theta_0)$  as a random variable representing whether user  $x$  is a strong interferer at time  $t$ , and  $Y_x^{t+\Delta t}$  a random variable representing the state of the same user at  $t + \Delta t$ , i.e.,

$$Y_x^{t+\Delta t} = f(x + \Delta X, \Theta + \Delta \Theta, \tilde{\Phi}^{t+\Delta t} \setminus (x + \Delta X, \Theta + \Delta \Theta), \Delta X_0, \Theta_0 + \Delta \Theta_0),$$

where  $\Delta X$ ,  $\Delta \Theta$  are random variables having the same distribution as  $\Delta X_i$  and  $\Delta \Theta_i$  respectively,  $Y_x^t$  and  $Y_x^{t+\Delta t} \in$

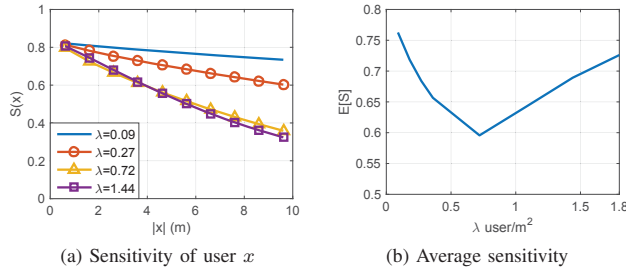


Fig. 6. (a) Sensitivity of users at different distance  $|x|$ , and (b) average sensitivity of a typical strong interferer  $E[S]$  for different user densities.

$\{0, 1\}$ . We define the *sensitivity* of an interferer originally located at  $x$  for an interval of length  $\Delta t$ ,  $S(x, \Delta t)$ , based on the autocorrelation of the state of the interferer at  $t$  and  $t + \Delta t$  as follows,

$$S(x, \Delta t) = \text{Corr}(Y_x^t, Y_x^{t+\Delta t}) = \frac{\text{Cov}(Y_x^t, Y_x^{t+\Delta t})}{\sigma_{Y_x^t} \cdot \sigma_{Y_x^{t+\Delta t}}}, \quad (3)$$

where  $\text{Cov}(Y_x^t, Y_x^{t+\Delta t}) = E[Y_x^t Y_x^{t+\Delta t}] - E[Y_x^t] E[Y_x^{t+\Delta t}]$ ,  $\sigma_{Y_x^t}$  and  $\sigma_{Y_x^{t+\Delta t}}$  are the variance of  $Y_x^t$  and  $Y_x^{t+\Delta t}$ ,  $S(x, \Delta t) \in [0, 1]$ . If  $S(x, \Delta t)$  is small, the autocorrelation of the user state is small and the channel sensitive to movements; if  $S(x, \Delta t)$  is close to 1, the autocorrelation is high and the interferer is stable.  $S(x, \Delta t)$  can be computed as used to obtain  $E[N_{\text{SI}}]$  and leveraging the simple mobility model. The details are omitted due to space constraints.

**Numerical results.** We present the numerical results on the sensitivity of LOS strong interferers for  $\Delta t = 1$  s in Fig. 6. We assume  $r_{\text{move}}$  is a function of  $\lambda$  and may decrease with user density, i.e.,  $r_{\text{move}}(\lambda) = \min(0.23, 0.6\sqrt{1/\lambda\pi})$  m, to capture the fact that users' local movements become limited as the distance among users becomes smaller. The range for rotation is  $48^\circ$ , i.e.,  $\omega = 24^\circ$ . Fig. 6(a) exhibits the sensitivity of users at different distances. As can be seen, distant interferers are more sensitive to perturbations than close by interferers. This supports the observation that close by users (interferers) will be robust to movements and learning the interference from close by neighbors is more reliable. Fig. 6(b) exhibits the sensitivity of a typical strong interferer,  $E[S]$ ,

$$E[S] = \frac{\lambda \int_{\mathbb{R}^2 \setminus b(0, r_{\min})} S(x, \Delta t) \cdot P_{\text{SI}}(x) dx}{E[N_{\text{SI}}]},$$

for different user densities, where  $P_{\text{SI}}(x)$  is the probability that the user located at  $x$  is a strong interferer of user at 0, which can be computed based on our blockage model. Strong interferers first become more sensitive to movements as  $S(x, \Delta t)$  decreases with  $\lambda$ . In highly dense scenarios, strong interferers are closer and the movements become limited, thus the strong interferers become more robust to user local movements.

#### IV. PERFORMANCE OF HIERARCHICAL WEARABLE MAC

In this section, we propose a simple hierarchical MAC protocol for dense wearable networks and study its performance.

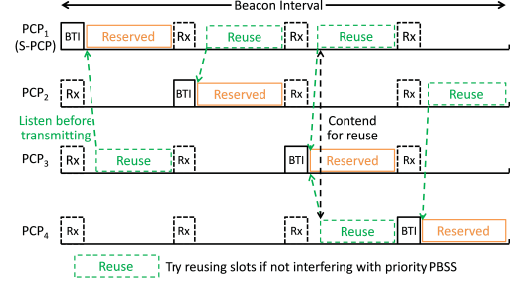


Fig. 7. Frame structure of clustering with Hierarchical Resource Reuse.

#### A. Hierarchical MAC for Wearable Networks

When centralized control is absent, hierarchical clustering and scheduling work as a viable solution to coordinating the multiple PBSSs, e.g., the distributed clustering in 802.11ad.

The hierarchical MAC consists of three parts, clustering, channel selection and scheduling at each PBSS. The cluster head synchronizes PBSSs in the cluster and schedules Beacon Transmission Intervals (BTIs) for each cluster member PBSS. Due to high user density and unstable channels, cluster head may not schedule the data transmissions for cluster members. Channel selection is mainly used to mitigate interference, either the cluster head selects a channel for all members in the cluster, or the PBSSs choose the channel to work on then form clusters on that channel. Clustering and channel selection help coordinate the PBSSs and are usually performed at a slower time scale. In each PBSS, the PCP schedules the data transmissions within the PBSS for each frame while trying to optimize reuse in dense scenarios.

Current standards leave open the question of how to form clusters and select channels according to the scenario. Another major problem is that reuse might be limited, e.g., PBSSs may not use the same slots and work in a time division multiple access (TDMA) like manner if they can hear others' beacons in 802.11ad.

For dense wearable networks, the basic principle underlying clustering is that the channels between cluster head and cluster members should be strong and stable. To better mitigate inter-cluster interference through channel selection, it is also desirable that cluster members share a similar set of strong interferers. Based on our analysis of channels and the above principles, a cluster shall consist of users in close proximity and operate in a channel distinct from that of nearby clusters.

To achieve better resource reuse within the cluster and meet the basic QoS requirements of each PBSS, we propose a hierarchical scheduling method shown in Fig. 7. Each PBSS is allocated a reserved slot where it has priority over the other PBSSs. Other PBSSs may however try to contend with other non-priority PBSSs to reuse slots if the their transmissions do not interfere with the transmissions of the priority PBSS.

#### B. Modeling Achievable Reuse for Hierarchical MAC

In this section we propose a model to compute the achievable reuse of clustering for dense wearable networks.

Consider the average time that a typical PBSS can perform a successful data transmission, denoted by Successful Transmission Time (STT), as the performance metric of interest. A PBSS interferes with another PBSS if the interference power it causes at the receiver is above a threshold  $\gamma_{\text{SI}}$ . We say two users interfere with each other if the interference power at either user exceeds  $\gamma_{\text{SI}}$ . A transmission is successful if there is no interferer. STT is then defined as follows,

$$STT = f_{\text{data}} \times p_{\text{access}} \times p_{\text{success}},$$

where  $f_{\text{data}}$  is the fraction of time reserved for data transmission,  $p_{\text{access}}$  is the probability that a PBSS may access the channel and does not interfere with other PBSSs within the same cluster, and  $p_{\text{success}}$  is the probability that a transmission is free from inter-cluster interference.

There are two types of transmissions, beacon and data transmissions. To account for the heterogeneity of devices, e.g., transmission capabilities and QoS requirements, we classify data transmissions of each PBSS into two categories, primary data transmissions with higher QoS requirements and highly directional antennas and secondary data transmissions associated with lower QoS requirements and less directional antennas.

**Modeling clustering and channel selection.** We assume that clusters are of the same size  $K$  and share  $M$  channels. Each cluster includes the nearest neighbors of the cluster head and when possible each cluster chooses to operate on different channels than closest neighboring clusters. In a typical cluster, we model the cluster head as located at the center while the other  $K - 1$  cluster members are its closest neighbors.

To obtain a tractable simple model, we assume the cluster members are uniformly distributed on a disc centered at the cluster head with a fixed radius  $R_{\text{cluster}}$ , see Fig. 8. Suppose user density on the disc is the same as  $\lambda$ , then the expected number of users on the disc should be equal to the number of cluster members,  $K - 1$ , i.e.,

$$\lambda\pi(R_{\text{cluster}}^2 - r_{\text{min}}^2) \approx K - 1,$$

$$R_{\text{cluster}} \approx \sqrt{\frac{K - 1}{\lambda\pi} + r_{\text{min}}^2}.$$

Channel selection is geared at ensuring neighboring clusters operate on different channels and thus effectively forms an inter-cluster interference protection region, see Fig. 8. An idealized protection area is modeled as a disc centered at the cluster head with a radius  $R_{\text{protect}}$ , where there are no inter-cluster interferers. Assume the fraction of clusters operating on each channel is equal, and the number of users in the protection area of each cluster is the same. We further assume the protection areas of clusters on the same channel are non-overlapping, then on average there should be  $M \cdot K$  users in the protection area. Suppose these users are uniformly distributed on the protection area with density  $\lambda$ , then we have under our idealized model,

$$\lambda\pi(R_{\text{protect}}^2 - r_{\text{min}}^2) \approx M \cdot K - 1,$$

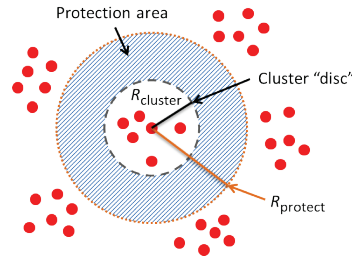


Fig. 8. Model of clustering and channel selection. Red circles represent users working on the same channel.

$$R_{\text{protect}} \approx \sqrt{\frac{M \cdot K - 1}{\lambda\pi} + r_{\text{min}}^2}.$$

We shall assume users outside the protection area can be modeled as following a HPPP with density  $\lambda$  and operating on a given channel with probability  $1/M$ . All PBSSs outside the protection region work independently.

**Modeling scheduling.** We assume there is at most one transmission in each PBSS in each slot. Let  $T_{\text{frame}}$  denote the length of a cluster shared frame and  $T_{\text{beacon}}$  denote the length of one BTI. The cluster head reserves exactly  $K$  BTIs in  $T_{\text{frame}}$  thus the proportion of data reserved for data transmission is given by

$$f_{\text{data}} = \frac{T_{\text{data}}}{T_{\text{frame}}} = \frac{T_{\text{frame}} - K \cdot T_{\text{beacon}}}{T_{\text{frame}}}.$$

In each BTI, exactly one PCP will transmit its beacon and the other devices will attempt to receive the beacon using omni-directional receive mode. The PBSSs are full-buffer and schedule primary transmissions a proportion  $\rho_{\text{primary}} \in [0, 1]$  of slots for data transmission and schedule secondary transmissions for the remaining  $\rho_{\text{secondary}} = 1 - \rho_{\text{primary}}$  slots.

We consider two types of scheduling within clusters: TDMA and Hierarchical Resource Reuse (HRR). In TDMA scheduling, PBSSs share the slots equally within the cluster and the fraction of time that a PBSS can access the channel in a frame is given by,

$$p_{\text{access}}^{\text{TDMA}} = f_{\text{data}}/K.$$

A PBSS schedules primary transmissions in  $\rho_{\text{primary}}f_{\text{data}}/K$  slots, and secondary transmissions in the rest  $(1 - \rho_{\text{primary}})f_{\text{data}}/K$  slots.

In HRR, each PBSS is allocated  $1/K$  of the slots where it is priority PBSS, i.e., having higher priority in scheduling. A PBSS first schedules primary transmissions in the reserved slots and schedules other transmissions by reusing slots allocated to other PBSSs. If  $\rho_{\text{primary}} \leq 1/K$ , the PBSS also schedules secondary transmissions in the allocated slots. Other PBSSs will try to reuse the slots if they do not interfere with the priority PBSS owning the slot. The probability that a PBSS can reuse a given slot is approximated by

$$p_{\text{access}}^{\text{reuse}} \approx (1 - p_{\text{SI}}^{\text{priority}}) \cdot \frac{1}{1 + \text{E}[N_{\text{intra-cluster}}^{\text{reuse}}]},$$

TABLE I  
THE PARAMETERS USED FOR MAC ANALYSIS

Parameter	Value
Frequency	60 GHz
M	4
$\lambda$	1 user/m <sup>2</sup>
$P_t$ (primary)	10 dBm
$P_t$ (secondary)	4 dBm
$\gamma_{SI}$	-78 dBm
$g_{\text{main}} (\beta = 60^\circ)$	5 dB
$g_{\text{side}} (\beta = 60^\circ)$	-5 dB
$g_{\text{main}} (\beta = 24^\circ)$	10 dB
$g_{\text{side}} (\beta = 24^\circ)$	-10 dB
$T_{\text{frame}}$	100 ms
$T_{\text{beacon}}$	2 ms

where  $p_{SI}^{\text{priority}}$  is the probability that the typical PBSS interferes with the priority PBSS considering the channel path loss and antenna gain,  $N_{\text{intra-cluster}}^{\text{reuse}}$  is number of non-priority PBSSs in the cluster, which do not interfere with the priority PBSS and contend with the typical PBSS to reuse the slot.

Denote by  $N_{\text{inter-cluster}}$  the number of inter-cluster interfering PBSSs. The activities of inter-cluster interferers are assumed to be mutually independent thus  $N_{\text{inter-cluster}}$  follows a Poisson distribution and the probability of a successful transmission is approximated as follows,

$$p_{\text{success}} = e^{-E[N_{\text{inter-cluster}}]}.$$

The distribution of  $N_{\text{inter-cluster}}$  is related to the transmission patterns of interfering PBSSs, which in turn depends on the location of PBSSs within the cluster. We use the transmission pattern of a user  $\frac{\sqrt{2}}{2}R_{\text{cluster}}$  away from the cluster head as the typical transmission pattern and all inter-cluster PBSSs have the same transmission pattern.

### C. Numerical Results and Discussion

In this section, we present the achievable STT of a representative user which is located between the center and the edge of the cluster at a distance  $\frac{\sqrt{2}}{2}R_{\text{cluster}}$  to the center. We assume the secondary transmissions use omni-directional antenna and low transmit power while primary transmissions use directional antenna with  $\beta = 60^\circ$ ,  $\rho_{\text{primary}} = 0.5$ . The parameters used are listed in Table I.

We begin by comparing our analytical model with simulation in Fig. 9. In our simulation, the locations of users follow a Matérn III process [19], i.e., users can not overlap each other. The blockage from other users follows the probabilistic model based on distance while self-blockage and antenna gain are calculated based on user locations and orientations and antenna directions. Users are first clustered using Affinity Propagation (AP) [20] based on a similarity metric between two users  $i$  and  $j$ , which is simply defined as the inverse squared distance, i.e.,  $d_{ij}^{-2}$ , where  $d_{ij}$  is the distance between user  $i$  and  $j$ . After clustering, the cluster heads hop among channels, attempting to minimize the sum similarity to inter-cluster PBSSs that are on the same channel. Channel selection is performed for a fixed number of rounds at which point cluster heads stop selecting channels. After clustering and channel selection,

each cluster schedules users either using TDMA or HRR. In HRR, each non-priority PBSS is assigned a random reuse-priority, and a non-priority PBSS user can reuse the channel if it does not interfere with the priority PBSS, nor other non-priority PBSSs which have higher reuse priority and do not interfere with the priority PBSS. As shown in Fig. 9, the simulation results for this more realistic network model, e.g., with real clusters, channel selection and scheduling, are in accordance with our simplified analytical model.

**Trade-offs associated with cluster size.** Fig. 9 exhibits how the STT changes with cluster size. STT first increases with cluster size, then saturates and decreases, indicating that while large clusters may provide good inter-cluster interference mitigation, they increase the contention between users within a cluster as well as signaling overheads thus may reduce the spatial reuse.

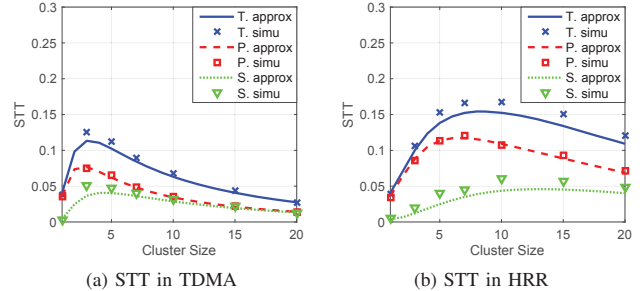


Fig. 9. Total STT (T.), STT of primary transmissions (P.) and STT of secondary transmissions (S.) in TDMA and HRR for different cluster sizes.

**Impact of transmission capability of devices.** Fig. 10 compare the STT when users have different beamwidths  $\beta$  for primary transmissions. As might be expected, the optimal cluster size maximizing STT is smaller when the transmissions are more directional. Results suggest that highly directional devices are less dependent on clustering to mitigate interference, thus users with highly directional devices may favor small clusters or be better off not joining clusters at all.

**Optimal cluster size v.s. user density.** In Fig. 11 we show how the cluster size maximizing the sum STT of primary and secondary transmissions changes with user density. When user

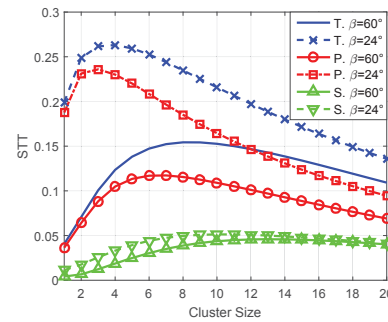


Fig. 10. Comparison of STT for networks with different beamwidths  $\beta$  for primary transmissions.

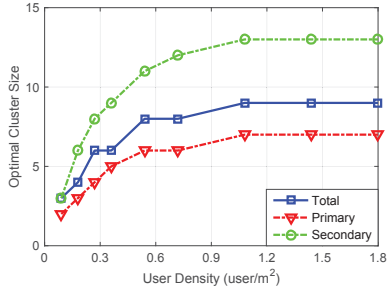


Fig. 11. Cluster size that maximizes STT for different user densities.

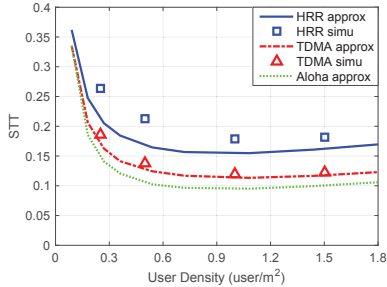


Fig. 12. STT in different user densities for different MAC protocols: Cluster+HRR, Cluster+TDMA and optimal Aloha.

density is high, the optimal cluster size does not change very much, indicating that the optimal cluster size is pretty robust to user density. However, as we have discussed, the transmission capabilities of users influence the optimal cluster size.

**STT v.s. user density.** In Fig. 12 we compare the STT for different MAC protocols and user densities. At each user density, the cluster size is chosen as the one that maximizes the STT. For Aloha, we assume users select channels randomly and the access probability is optimized to maximize the total STT. We observe that clustering and reuse provide moderate gains in STT, partly due to beacon overheads. The STT of users remains constant with user densities, indicating that the per user throughput scales with user density at high densities. Combined with observation that optimal cluster size is robust, we can see that MAC is scalable in dense wearable networks. Our result here is different from the existing scaling results on ad hoc networks in that the transmit power and the signal strength do not change with density.

## V. CONCLUSION

Our analysis of character of interference and MAC performance in dense mm-wave wearable networks suggests such networks might be quite viable. Blockage and directionality help limit the number of strong interferers to a few that are close by and stable. For a relative stationary network, clustering with resource reuse is a viable solution to coordinating PBSS transmissions. An ideal cluster protocol should be able to adapt to user transmission capabilities and QoS requirements. More importantly, the overhead and performance of MAC scale well at high densities. In fact when designing and evaluating a MAC, one may want to focus on the most

challenging scenario at which one has a moderate density of users.

## ACKNOWLEDGEMENT

The research in this paper was supported in part by NSF Grant CNS-1343383 and an Intel grant.

## REFERENCES

- [1] "Smart Wearable Devices: Fitness, Glasses, Watches, Multimedia, Clothing, Jewellery, Healthcare & Enterprise 2014-2019," *Juniper Research*, Aug. 2014.
- [2] "IEEE Standard for Information Technology Telecommunications and Information Exchange between Systems Local and Metropolitan Area Networks Specific Requirements. Part 11: Wireless MAN Medium Access Control (MAC) and Physical Layer (PHY) Specifications Amendment 3: Enhancements for Very High Throughput in 60 GHz Band," IEEE Standard 802.11ad, 2012.
- [3] "IEEE Standard for Information Technology Telecommunications and Information Exchange between Systems Local and Metropolitan Area Networks Specific Requirements. Part 15.3: Wireless Medium Access Control (MAC) and Physical Layer (PHY) Specifications for High Rate Wireless Personal Area Networks (WPANs) Amendment 2: Millimeter-Wave-Based Alternative Physical Layer Extension," IEEE Std 802.15.3c, 2009.
- [4] "High Rate 60 GHz PHY, MAC and PALs," ECMA Standard 387, 2010.
- [5] C. Gustafson and F. Tufvesson, "Characterization of 60 GHz Shadowing by Human Bodies and Simple Phantoms," *Antennas and Propagation (EUCAP)*, 6th European Conference on, 2012.
- [6] K. Venugopal, M.C. Valenti and R.W. Heath, "Interference in Finite-Sized Highly Dense Millimeter Wave Networks," *Information Theory and Applications Workshop*, Feb. 2015.
- [7] G. George and A. Lozano, "Performance of enclosed mmWave wearable networks," in *IEEE Int'l Workshop on Computational Advances in Multi-Sensor Adaptive Processing (CAMSAP 15)*, Dec. 2015.
- [8] T. Bai and R.W. Heath Jr., "Coverage and rate analysis for millimeter wave cellular networks," *IEEE Trans. Wireless Comm.*, vol. 13, no. 9, Sep. 2014.
- [9] S. Collonge, G. Zaharia and G.E. Zein, "Influence of human activity on wide-band characteristics of the 60 GHz indoor radio channel," *IEEE Trans. Wirel. Commun.*, vol. 3, no. 6, pp. 2369-2406, 2004.
- [10] I. Kashiwagi, T. Taga and T. Imai, "Time-varying path-shadowing model for indoor populated environments," *IEEE Trans. Veh. Technol.*, vol. 59, no. 1, Jan. 2010.
- [11] S. Singh, F. Ziliotto, U. Madhow, E. M. Belding and M. Rodwell, "Blockage and Directivity in 60 GHz Wireless Personal Area Networks: From Cross-Layer Model to Multihop MAC Design," *IEEE J. Sel. Areas Commun.*, vol. 27, no. 8, Oct. 2009.
- [12] E. Shihab, L. Cai, and J. Pan, "A distributed asynchronous directional-to-directional MAC protocol for wireless ad hoc networks," *IEEE Tans. Veh. Tech.*, vol. 58, no. 9, pp. 5124-5134, Nov. 2009.
- [13] S. Singh, R. Mudumbai, and U. Madhow, "Distributed coordination with deaf neighbors: efficient medium access for 60 GHz mesh networks," in *Proc. IEEE INFOCOM*, San Diego, CA, 2010, pp. 1-9.
- [14] W. Feng, Y. Li, D. Jin and L. Zeng, "Inter-Network Spatial Sharing with Interference Mitigation Based on IEEE 802.11ad WLAN System," *Globecom 2014 workshop - telecommunications standards - from research to standards*
- [15] Z. He, S. Mao and T.S. Rappaport, "On Link Scheduling Under Blockage and Interference in 60-GHz Ad Hoc Networks," *IEEE Access*, vol. 3, pp. 1437-1449, Aug. 2015.
- [16] K. Sato *et al.*, "Measurements of Reflection and Transmission Characteristics of Interior Structure of Office Building in the 60-GHz band," *IEEE Trans. Antennas Propag.*, vol. 45, no. 12, pp. 1783-1792, Dec. 1997.
- [17] J. F. C. Kingman, "Poisson Processes," New York: The Clarendon Press Oxford Univ. Press, 1993.
- [18] F. Baccelli and B. Błaszczyszyn, "Stochastic geometry and wireless networks, volume I - theory," *Foundations and Trends in Networking*, vol. 3, no. 3-4, pp. 249-449, 2009.
- [19] B. Matérn, "Spatial Variation," *Lecture Notes in Statistics*, vol. 36, 1986.
- [20] B.J. Frey and D. Dueck, "Clustering by Passing Messages Between Data Points," *Science* 315 (2007) 972-976.